9-2013

KSHV encoded Rta induces cell cycle arrest

Pankaj Kumar
University of Nebraska- Lincoln

Charles Wood
University of Nebraska- Lincoln, cwood1@unl.edu

JVI Accepts, published online ahead of print on 25 September 2013
J. Virol. doi:10.1128/JVI.02540-13

Kaposi's Sarcoma-associated Herpesvirus Transactivator Rta Induces Cell Cycle Arrest in G0/G1 Phase by Stabilizing and Promoting Nuclear Localization of $p27^{kip}$

Running Title: KSHV encoded Rta induces cell cycle arrest

Pankaj Kumar and Charles Wood#

Nebraska Center for Virology and the School of Biological Sciences, University of Nebraska-Lincoln, Lincoln NE 68583

Word Count

Abstract: 233

Text: 5958

Correspondent Footnote

102C Morrison Center

4240 Fair Street

University of Nebraska Lincoln

Lincoln NE 68583

USA

cwood1@unl.edu

Abstract

The Kaposi's sarcoma-associated herpesvirus (KSHV) encoded immediate early gene, replication and transcription activator (K-Rta) is a key viral protein that serves as the master regulator for viral lytic replication. In this study, we investigated the role of K-Rta in cell cycle regulation and found that the expression of K-Rta in doxycycline (Dox)-inducible BJAB cells induced cell cycle arrest in G0/G1 phase. Western blot analysis of key cell cycle regulators revealed that K-Rta-mediated cell cycle arrest was associated with a decrease in Cyclin A and phosphorylated Rb (pS807/ pS811) protein levels, both markers of S phase progression and an increase in protein levels for p27, a cyclin-dependent kinase inhibitor. Further, we found that K-Rta does not affect the transcription of p27 but regulates p27 at the post-translational level by inhibiting its proteosomal degradation. Immunofluorescence staining and cell fractionation experiments revealed largely nuclear compartmentalization of p27 in K-Rta expressing cells demonstrating that K-Rta not only stabilizes p27 but also modulates its cellular localization. Finally, shRNA knockdown of p27 significantly abrogates cell cycle arrest in K-Rta expressing cells supporting its key role in K-Rta mediated cell cycle arrest. Our findings are consistent with previous studies which showed that expression of immediate early genes of several herpes viruses including HSV, EBV and CMV results in cell cycle arrest at the G0/G1 phase, possibly to avoid competition of resources needed for host cell replication during the S phase.

Introduction

Kaposi's sarcoma-associated herpesvirus (KSHV), also known as Human herpesvirus-8 (HHV-8) is a member of gammaherpesvirus family that includes Epstein Barr Virus (EBV), Herpesvirus saimiri (HVS) and Murid herpesvirus 68 (MHV 68) (1). KSHV is the etiological agent of Kaposi's sarcoma (KS), the most common tumor associated with HIV infection and for at least two other malignancies, pleural effusion lymphoma (PEL) and multicentric Castleman's disease (MCD) (2-4). Like all herpesviruses, the life cycle of KSHV consists of latent and lytic phases. The latent phase is characterized by a restricted pattern of viral gene expression that facilitates the evasion of immune surveillance and the establishment of lifelong persistent infection. The lytic phase drives the replication cycle and a majority of the viral genes are expressed in this phase. This phase mainly allows for the spread of the virus in the infected individual. A growing body of research suggests that both latent and lytic replication phases play an important role in the pathogenesis of KS (5).

The transition from latency to lytic replication is controlled by the KSHV replication and transcription activator (K-Rta) gene, an immediately early gene encoded by open reading frame 50 (ORF50). K-Rta expression has been found to be essential and sufficient to trigger lytic replication by activating the lytic gene expression cascade (6-8). Genetic knockout of K-Rta resulted in a null phenotype in viral DNA synthesis and in virus production (9). K-Rta is a 691-amino acid (aa) long transcriptional factor that contains an N-terminal DNA-binding domain and a C-terminal activation domain. K-Rta can trigger KSHV lytic reactivation via transcriptional activation of a number of viral lytic promoters, by either binding directly to the promoter DNA or indirectly via interaction with cellular DNA binding proteins (10-15).

There is a complex interplay between herpesvirus lytic replication and host cell cycle arrest. Previous studies investigating the role of cell cycle in herpesvirus lytic replication

63 suggested that host cell cycle arrest precedes the induction of lytic cycle and essentially
64 determines whether immediate early gene expression is initiated or not (16). However, current
65 research increasingly support the idea that cell cycle arrest follows lytic cycle induction and is a
66 direct consequence of immediate early gene expression (17-19). It is hypothesized that arresting
67 cells during early lytic replication may be an evolutionary common strategy employed by
68 herpesviruses to avoid competition of resources required for viral DNA replication with the host
69 in the S phase, or it may serve to prevent premature apoptosis during lytic replication (20). This
70 is in contrast to small DNA viruses, especially those lacking their own polymerase like SV40 and
71 adenoviruses which actively drive host cells into S phase of the cell cycle in order to replicate
72 their genome at the same time with host DNA synthesis. Arresting cell growth early during
73 infection/reactivation may also be a strategy to avoid being killed by cytotoxic T cells as it has
74 been reported that non-cycling cells are refractory to killing by cytotoxic T cells (21).
75 To date, several herpesvirus-encoded proteins have been identified that participate in
76 arresting host cell growth. These proteins are either virion components and/or immediate early
77 (IE) transcriptional factors. For example, the IE product of herpes simplex virus, ICPO has been
78 found to arrest cell cycle in G1 phase by both p53 mediated and p53 independent pathways (22,
79 23) . In the case of EBV, immediate early product, Zta can induce host cell cycle arrest by
80 stabilizing p53 and p27, and also through repressing the expression of c-myc (24, 25).
81 Furthermore it has been shown that Zta may cooperate with host transcriptional factor C/EBP to
82 upregulate p21, which in turn results in cell cycle arrest (26).
83 Among the characterized early genes of KSHV, K8 or K-bZIP protein, a functional
84 homologue of EBV's immediate early Zta protein was shown to arrest PEL cells in G1 phase
85 during lytic cycle by up regulating C/EBP and p21 proteins (27). K8 was also found to inhibit
86 kinase activities of CDK2 by directly binding through its bZIP domain (17). However the role of

87 KSHV encoded ORF50/K-Rta, one of the first genes transcribed and the central regulator for the
88 initiation of lytic replication cycle, in cell cycle regulation has not been evaluated. In the present
89 study, we demonstrated that K-Rta induces cell cycle arrest in an inducible BJAB cell model and
90 this growth arrest is mediated by elevated levels of p27, a central cyclin-dependent kinase
91 inhibitor (CDKI). Our results shed new light on the biological function of K-Rta as a key cell
92 cycle regulator early on during viral reactivation, in addition to being a transcriptional regulator.

Materials and Methods

Cell culture plasmids and transfection. 293T cells, 293 based doxycycline-inducible K-Rta cell line (TREx293Rta) (provided Dr Yoshihiro Izumiya, University of California at Davis, California) and Vero cells were cultured in Dulbecco's modified Eagle's medium (DMEM; Invitrogen, Carlsbad CA) supplemented with 10% fetal bovine serum (FBS; HyClone, Logan, UT) and 100 µg/ml penicillin-streptomycin (Mediatech). DG75 is an EBV-negative Burkitt's lymphoma (BL) derived B-cell line (provided by Dr. Luwen Zhang, University of Nebraska-Lincoln, Lincoln NE). It was grown in RPMI 1640 medium (Gibco BRL) supplemented with 10% FBS and 100 µg/ml penicillin-streptomycin. TRExBJABRta and TRExBJAB cells are BJAB (EBV and KSHV negative B-cell line) derived cell lines with or without doxycycline-inducible K-Rta gene. They were provided by Dr Jae Jung (University of Southern California, Los Angeles, CA) (28) and were grown in RPMI 1640 medium supplemented with 10% FBS, 100 µg/ml penicillin-streptomycin and 200 µg/ml of hygromycin B. KSHV-positive and EBV-negative B cell lines, BC3 cells (ATCC, USA) and Cro6 (29) (provided by Dr. Luwen Zhang, University of Nebraska-Lincoln, Lincoln NE) were grown in RPMI 1640 medium (ATCC, USA) supplemented with 20% FBS and 100 µg/ml penicillin-streptomycin. Human Microvascular Endothelial Cells (HMVEC) cells were grown in endothelial basal medium-2 (EBM-2) (Lonza, Boston, MA) supplemented with 10% fetal bovine serum (FBS), 100 µg/ml penicillin-streptomycin, 0.01 µg/ml epidermal growth factor, and 1 µg/ml hydrocortisone (30). All cultures were incubated at 37°C with 5% CO_2.

K-Rta expression plasmid (pCMVtagORF50), which encodes Flag-tagged full length Rta and pCMVtagORF50 (1-527), which encodes truncated K-Rta (amino acid 1 to 527), were described previously (31). The transfection of 293T cells and Vero cells was carried out using Lipofectamine 2000 (Invitrogen) or Fugene 6 (Promega) according to the manufacturer's

recommendations. The transfection of DG75 was carried out using the nucleofection protocol according to the manufacturer's protocols (Solution V and program O-006, Amaxa Biosystems). Cell Cycle analysis. Cell cycle profiles were analyzed by flow cytometry with standard propidium iodide (PI) staining methods (32). Asynchronized and synchronized cells were harvested at given time points, washed once with PBS and fixed in 70% ethanol at -20°C. After collection of all time points, the cells were washed with PBS twice and were resuspended in PBS containing PI (Roche) at a final concentration of 10 µg/ml and RNase A (20 µg/ml). The samples were kept at RT for 30 min in dark and 20,000 events per sample were acquired using FACS Calibur flow cytometer (BD Biosciences). The data was analyzed using Modfit LT version 2.0 software (Verity Software House Inc.).

RNA extraction and RT-PCR. Total cellular RNA was extracted using an RNeasy kit (QIAGEN) according to the manufacturer's procedure. RNA samples were digested with DNase (Invitrogen) to remove any residual DNA. Total RNA (2 µg) was used for reverse transcription (RT) using oligo(dT) as primers and Superscript II reverse transcriptase kit (Invitrogen, Inc., Carlsbad, CA) according to the manufacturer's instructions. The primers used for the mRNA quantitation were p27 (F) 5-CGTCAAACGTAAACAGCTCG-3 and p27 (R)- 5-CATTCCATGAAGTCAGCGAT-3, ORF50 (F)- 5-CAAACCCCATCCCAACAT-3 and ORF50 (R)- 5-AGTAATCACGGCCCCTT-3, GAPDH (F) - 5-CCATGGAGAAGGCTGGGG-3 and GAPDH (R)- 5-CAAAGTTGTCATGGATGACC-3. These target genes were amplified using the iQ SYBER green real time master mix (BioRad) in a BioRad iCyclerIQ thermocycler. All reactions were performed in triplicate using the following conditions: 50°C for 2 min, 95°C for 10 min, 40 cycles of 95°C for 15 sec and 60°C for 1 min. Melting-curve data for all the samples were obtained to ensure specific amplification. All reactions were performed in triplicate and included no-template controls for each gene. The experiments were repeated 2 times using

141 samples in triplicate. Relative gene expression was calculated using delta-delta-CT method (33).
142 For calculating relative mRNA levels, the CT (threshold cycle) value of each gene was
143 normalized to the CT value of GAPDH, and the normalized CT values from samples were
144 compared to those of the control samples (untreated).
145 Immunoprecipitation and immunoblot analysis. Total cell lysates for immunoprecipitation
146 and western blotting were prepared in radioimmunoprecipitation assay buffer (RIPA) (50 mM
147 Tris-HCl (pH 8.0), 150 mM NaCl, 1 mM EDTA, 1% NP-40) supplemented with protease and
148 phosphatase inhibitor cocktail (Pierce). The lysates were kept in ice for 30 min with occasional
149 vortexing. Finally, the lysates were centrifuged for 15 min at 13,000 x g at 4°C and the
150 supernatant was collected. Cytosolic and nuclear proteins were extracted from TRExBJABRta
151 cells using Sigma-CelLytic™ NuCLEAR™ Extraction Kit using manufacturer's protocol. The
152 protein concentration was measured using a BCA protein kit (Pierce, Rockford, IL). For
153 immunoprecipitation, equal amount of lysate from each treatment was precleared with 20 µl of
154 Protein A/G Sepharose (1hr, 4°C). Five percent of the precleared lysate was saved as input
155 control and total amount of p27 was captured by incubating with 2 µg of anti-p27 (SC-1641;
156 Santa Cruz) antibody overnight at 4°C. Immune complexes were captured with 30 µl of a 1:1
157 mixture of Protein-A and Protein-G Sepharose beads (Pierce, Rockford, IL) for 2 hrs. The beads
158 were then pelleted and washed three times with ice-cold RIPA buffer. The immunoprecipitated
159 proteins were eluted by heating in 2X sample buffer and subjected to immunoblotting.
160 For immunoblotting, equal amounts of total proteins (40 µg) were separated by sodium
161 dodecyl sulfate polyacrylamide gel electrophoresis (SDS-PAGE) and subsequently transferred to
162 nitrocellulose membrane using standard methods. After blocking with 5% non-fat dry milk in
163 Tris-buffered saline (TBS) (20 mM Tris pH-7.4, 137 mM NaCl) containing 0.01% Tween-20
164 (TBST) for 1 hr, the membrane was incubated with primary antibody overnight at 4°C.

Following washing with TBST three times, the membrane was incubated with horse peroxidase conjugated goat anti-rabbit/mouse secondary antibody (1:10000, Pierce) or infrared-tagged secondary antibodies (1:10000, Licor Inc., Lincoln, NE) for 30 min. Antibody binding was detected using SuperSignal West Dura Extended Duration Substrate kit (Pierce) or using an Odyssey imager. Image analysis and quantification of immunoreactive bands was performed using the Odyssey Infrared Imaging System application software (LiCor Inc., Lincoln, NE) or NIH ImageJ software.

Following antibodies were used in the present study: anti-rabbit K-Rta antibody was a kind gift from Dr Izumiya (UC Davis, California) and was used at a dilution of 1:5000. The anti-rabbit p27 (SC-528), anti-mouse p27 (SC-1641), anti-rabbit p21 (SC-397), anti-rabbit Rb (pS807/pS811) (BD558389), anti-rabbit Cyclin A (SC-751), anti-mouse GAPDH (SC-32233), anti-mouse Ub (SC-8017), anti-rabbit Skp2 (H-435), anti pp27-T187 (Ab75908), anti-mouse TATA binding protein (Ab818), anti-mouse α tubulin (SC-5286) were used at 1:1000 dilution in TBST.

Protein stability test. Exponentially growing TRExBJABRta cells were cultured in the presence of doxycycline (DOX) for 24 hrs. DOX treated and untreated cells were treated with 50 μg/ml cyclohexamide (CHX) (Sigma-Aldrich, St. Louis, MO). The cells were harvested at indicated time points after CHX treatment and cell lysates were subjected to Western blot analysis. Band intensities were quantitated using Odyssey 3.0 software provided by Odyssey imager (LiCor Inc., Lincoln, NE) and the half-life of p27 protein was calculated from the slope of the curve.

Immunofluorescence assay. TRExBJABRta cells were treated with doxycycline for 48 hrs. The cells were fixed with 4% paraformaldehyde for 20 min, permeabilized with 0.2% Triton X-100 in phosphate buffered saline (PBS) for 10 minutes, and blocked for 30 min with 2% bovine serum albumin (BSA) in PBS at room temperature (RT). After incubation with primary

antibodies [anti-p27 mouse monoclonal (BD) and anti-rabbit K-Rta] both at 1:250 dilution in 2% BSA for 2 hrs at RT, the cells were incubated with anti-mouse Alexa-Fluor-488 and anti-rabbit Alexa-Fluor-647 conjugated secondary antibodies (1:1000) for 1 hour at RT. This was followed by three washes with PBS. The last wash contained 4',6-diamidino-2-phenylindole (DAPI) (Calbiochem) to counterstain nuclei. The localization of K-Rta/p27 and DAPI stained nuclei were visualized by confocal microscopy.

Lentivirus-based short hairpin RNAs (shRNA) knockdown of p27. To establish p27 knockdown cell line, plasmids encoding p27 shRNA (1 and 2) and scrambled negative control shRNA (1 and 2) were purchased from Origene and were transfected into TRExBJABRta cells using the Nucleofector kit T from Lonza (Walkersville, MD) according to the manufacturer's procedure (Program- G-016). The transfected cells were selected with puromycin (1 µg/ml) for 3 weeks.

Lentivirus vector expressing full length K-Rta, virus production and transduction of HMVEC cells. To generate a lentiviral vector expressing KSHV full length Rta, the coding sequence was cloned into pLVX-AcGFP1 (Clontech). The VSV-G-pseudotyped lentiviral particles were produced by transient cotransfection of 293T cells as described (34). Briefly, 5-6 x10^6 HEK293T cells were co-transfected with 18 µg of K-Rta expressing transfer vector (pLVX-Rta), 12 µg packaging vector psPAX2, and 6 µg of envelope vector pHEF-VSVG per 10 cm diameter plate at a 3:2:1 mass ratio by using standard calcium phosphate co-precipitation method. Eight hours post-transfection the media was replaced with DMEM supplemented with 10% FBS. The medium containing the virus was harvested 48 hours post-transfection, filtered through 0.45 µm pore filter and concentrated by ultracentrifugation at 4°C for 2 hrs at 25,000 rpm with T-865 rotor (Sorvall). Pellets were gently resuspended in DMEM and kept over-night at 4°C. The viral titers of concentrated pseudotyped lentiviruses were determined by transducing

213 3×10^5 293T cells seeded in one well of a 6-well plate in 4 ml of medium containing 8 µg/ml of
214 polybrene (Sigma). The media was replaced after 6 hrs. After 48 hours the number of cells
215 expressing GFP was determined using flow cytometry. The viral titers were calculated using the
216 formula: N×M / V where N is the number of target cells used for infection, M is % GFP
217 expressing cells, and V is the volume of concentrated virus used in ml.
218 Statistical Analysis. All data analysis was done using SPSS software (v11). Comparison of
219 mean number of cells was done using Student's t-test. All p-values ≤0.05 were considered
220 significant.

221 Results

222 Expression of K-Rta induces cell cycle arrest in G1 phase: Earlier investigations have
223 reported that TPA-induced reactivation of KSHV results in cell cycle arrest in G1 phase of the
224 treated cells and implicated early-lytic gene product K-bZIP for the induction of cell cycle arrest
225 (17). Indeed TPA treatment of asynchronously growing BC3 cells (KSHV positive latent B-cell
226 line) resulted in a marked increase of cells in the G1 fraction at 24 hrs after treatment, from 37%
227 (before treatment) to 56.5%. This increase in proportion of cells arrested in G1 phase was also
228 noted after TPA treatment of another KSHV positive latent B-cell line, Cro6, with a significant
229 increase from 55.6% (before treatment) to 70.5% at 24 hrs post treatment. However TPA
230 induced G1 arrest was not observed in KSHV negative control B-cell line DG75, at 24 hrs post
231 TPA treatment (Fig. 1). These results confirmed previous findings that KSHV lytic reactivation
232 arrests naturally infected B cells in G1 phase.

233 Since G1 arrest is favored after lytic replication, we sought to investigate whether any
234 other immediate early genes besides K-bZIP was involved in cell cycle arrest. We hypothesized
235 that K-Rta being the central regulator of viral lytic cycle and one of the very first genes to be
236 transcribed following reactivation may work in concert with K-bZIP to arrest cell cycle in G1
237 phase. To investigate K-Rta's role in cell cycle regulation, we utilized TRExBJABRta cells in
238 which myc-tagged full length K-Rta gene is integrated into the chromosomal DNA under the
239 control of a tetracycline-inducible promoter. Asynchronously growing exponential cultures of
240 TRExBJAB (Control) and TRExBJABRta were synchronized in G0/G1 phase by serum
241 starvation. The cells were released from growth arrest with the addition of medium containing
242 10% serum along with doxycycline. We then quantitated the fraction of cells in different phases
243 of cell cycle by flow cytometry at 24, 48 and 72 hrs post Dox treatment for both TRExBJAB and
244 TRExBJABRta cells. The fraction of cells arrested in G0/G1 phase after 24 hrs of serum

starvation treatment was about 53% for both cell lines. Serum starvation for extended time was avoided as it affected cell viability. The cell cycle profiles of both cell lines were similar following release from serum starvation without Dox treatment and showed enrichment of cells in S phase over time (Data not shown). Interestingly cell cycle profile clearly showed a significant increase in the number of cells arrested at G1 phase in TRExBJABRta cells compared to control TRExBJAB cells at 48 hrs ($p=0.006$) and 72 hrs ($p<0.001$) post Dox treatment (Fig. 2A). In contrast, there were more cells in S phase for TRExBJAB cells after 48 and 72 hr of Dox treatment, demonstrating that doxycycline alone has little or no effect on cell cycle progression following the release of cell cycle arrest in the absence of K-Rta. A significant arrest in G1 phase was also noted for Dox treated TREx293Rta cells at 72 hrs post treatment compared to untreated cells ($p <0.001$) (Fig. 2B) further supporting the data observed in BJAB cells. These results clearly show that the expression of K-Rta alone can induce cell cycle arrest in G1 phase.

K-Rta expression led to a decrease in phosphorylated Rb and a parallel increase in $p27^{kip1}$ protein levels: To explore the underlying mechanism of K-Rta mediated cell cycle arrest, the expression kinetics of key cell cycle regulators were analyzed by western blotting. Whole cell lysates were prepared from Dox treated and untreated TRExBJAB and TRExBJABRta cells. First we investigated the phosphorylation status of Retinoblastoma (Rb) protein, a critical negative regulator of the cell cycle that undergoes differential phosphorylation during the cell cycle (35). In early G1 phase Rb is largely dephosphorylated and bound to E2F family of transcriptional factors, forming a repressor complex. However, upon phosphorylation by Cdk4/6/cyclin D complex during early G1 phase and further by Cdk2/cyclin E during late G1 phase, Rb dissociates from E2F, thus activating the expression of proteins needed for S-phase entry and progression (35). We examined the status of Rb phosphorylation using an antibody that recognizes Rb phosphorylated at Ser807/Ser811. These sites are the target sites of Cdk4/6/cyclin

D complex during G1 phase. Induction of K-Rta in TRExBJABRta cells resulted in a significant decrease in the phosphorylated levels of Rb, most notably at 48 and 72 hrs post Dox treatment (Fig. 3A). The results were markedly different in Dox untreated TRExBJABRta, which displayed a significant increase in the levels of phosphorylated Rb in a time dependent manner that reached peak expression by 48 hrs, indicating that most of these cells were actively progressing through the cell cycle. In control TRExBJAB cells, the levels of phosphorylated Rb increased in a time dependent manner following release from cell cycle arrest, irrespective of Dox treatment suggesting that Dox treatment alone did not affect the normal cell cycle progression. Cyclin A is useful marker for S phase whose expression increases during cell cycle progression (36). Cyclin A expression in both cell lines with or without Dox treatment followed the expression kinetics similar to phosphorylated Rb.

Since the activities of G1 cyclin-CDK complexes are mainly regulated by Cip/Kip family of Cyclin dependent kinase inhibitors (CDKIs), we aimed to evaluate the expression profile of p21 and p27, two central regulators of cell cycle progression that inhibit a broad range of cyclin Cdk complexes. The levels of p27 significantly increased over time in Dox treated TRExBJABRta cells but the kinetics of p27 protein accumulation lagged by about 24 hrs following the expression of Rta in TRExBJABRta cells, reaching maximum levels at 48 hrs (~5X above background) whereas in untreated cells, p27 levels decreased in a time dependent manner. In TRExBJAB cells, the expression kinetics of p27 was similar in both Dox treated or untreated cells and was consistent with those described for cells entering S phase following cell cycle arrest in G1 phase. The levels of p21 remained largely unchanged during the course of experiment for both cell lines irrespective of Dox treatment. Since p21 is a direct transcriptional target of p53, we also investigated the expression levels of p53 and found no significant change in the relative levels of p53 in both cell lines with or without Dox treatment (data not shown).

These results demonstrated that K-Rta-mediated cell cycle arrest in BJAB cells does not involve p21 and is associated with a decrease in Rb phosphorylation and a parallel increase in p27 levels.

We also examined the expression of p27 in TPA treated BC3 cells and found that p27 levels increased in a time dependent manner following reactivation (Figure 3B). This increase in p27 levels was not observed in TPA treated DG75 cells. Although this increase in p27 levels in TPA treated BC3 cells does not directly implicate K-Rta but it does show that cell cycle arrest during reactivation of KSHV from a latently infected B cell line is associated with an increase in p27 levels.

To ensure that K-Rta mediated up regulation of p27 in BJAB cell line was not a cell type specific effect, we transiently transfected or transduced K-Rta in DG75, Vero cells and HMVEC cells respectively and checked the levels of p27 at 36 hours post-transfection/transduction by western blotting (Figure 3C) while the cells were actively growing at log phase. We found increased levels of p27 in cells that were transfected or transduced with K-Rta compared to cells that were transfected/transduced with vector or control virus. These results suggest that increase in p27 levels following K-Rta expression is not unique to BJAB cells.

K-Rta does not affect p27 at the transcriptional level: Since K-Rta is a transcriptional factor and has the ability to regulate the expression of cellular genes (37); we investigated the possibility whether the increased level of p27 in K-Rta expressing cells is due to transcriptional up regulation of p27 by K-Rta. Real time PCR was carried out with RNA samples extracted from Dox treated and untreated cells. As shown in figure 4A, the level of p27 mRNA after normalization with GAPDH showed no significant difference before and after K-Rta induction. The data suggest that the up regulation of p27 in K-Rta expressing cells is not due to increased p27 mRNA expression. These results were also supported by increased p27 levels observed in cells transiently transfected with K-Rta lacking the transactivation domain, suggesting that K-Rta

317 is not directly acting on p27 at the transcriptional level or the ability of K-Rta to upregulate p27
318 is independent of its transactivation function (Fig. 4B).
319 K-Rta expression results in stabilization of p27: Since p27 is mainly regulated at the post-
320 translational level via the ubiquitin-proteasome pathway (38, 39), we examined the effect of K-
321 Rta on the half-life of p27. Protein synthesis was blocked in K-Rta expressing BJAB cells by
322 cycloheximide and p27 protein levels were quantitated at various time intervals by
323 immunoblotting (Fig. 5A). As a control, we also followed p27 levels in Dox untreated
324 TRExBJABRta cells. In control cells, the half-life of p27 was found to be approximately 4.1 hrs
325 but in K-Rta expressing cells the half-life of p27 increased to approximately 7.3 hrs. The data
326 suggest that upregulation of p27 in K-Rta expressing cells is most likely mediated by changes in
327 protein stability. Next, we investigated the possibility whether reduced poly-ubiquitination of
328 p27 in K-Rta expressing cells is responsible for increased levels of p27. Poly-ubiquitination of
329 the p27 was assessed by immunoprecipitating p27 from Dox treated and untreated
330 TRExBJABRta cells followed by immunoblotting (Fig. 5B). As expected, there was an increase
331 in p27 levels in K-Rta expressing cells in both lysate and immunoprecipitated lanes, however we
332 detected decreased levels of ubiquitinated p27 in Dox-treated TRExBJABRta cells as evidenced
333 by a reduction of the smear of high molecular weight p27 bands as compared to the uninduced
334 Dox lane. These results suggest that the expression of K-Rta increases p27 stability by inhibiting
335 the poly-ubiquitination and subsequent proteasomal degradation.
336 K-Rta promotes nuclear localization of p27: The activity of p27 is also regulated by its
337 subcellular localization as it shuttles between nucleus and cytoplasm during the cell cycle (40).
338 p27 is exclusively nuclear during G0/G1 phase but is exported to the cytoplasm in response to
339 proliferating signals. Since the subcellular localization of p27 is inherently linked to the
340 regulation of p27 activity, we determined whether K-Rta is modulating the subcellular

341 localization of p27. The localization of endogenous p27 was investigated in Dox treated and
342 untreated TRExBJABRta cells by indirect immunofluorescence assay. Figure 6A shows a
343 representative field of immunostaining. As expected, intense staining suggesting higher p27
344 expression levels were observed in most K-Rta expressing cells. Further, the staining for p27 was
345 predominantly nuclear and colocalized with K-Rta. In most of the untreated TRExBJABRta
346 cells, the staining for p27 was less intense and mostly diffuse. In order to confirm the effects of
347 K-Rta on p27 localization observed in immunofluorescence assay, we performed cell
348 fractionation to determine the levels of p27 in nuclear and cytosolic extracts of untreated and
349 treated TRExBJABRta by western blot (Fig. 6B). We found a significant fraction of p27 in the
350 nuclear extracts (normalized to the total p27 levels) of K-Rta expressing BJAB cells (43% vs.
351 14%) compared to the control cells. These results demonstrate that in addition to increased
352 stability of p27, modulation of the intracellular localization of p27 also occurred in K-Rta
353 induced G1 arrest.
354 K-Rta induced cell cycle arrest coincides with down regulation of Skp2: Multiple
355 degradation pathways that regulate p27 protein levels have been characterized in recent years
356 (39). One of the best-understood pathways for degradation of p27 is mediated by SCF/Skp2
357 complex in late G1 phase and early S phase (41). CDK2-dependent phosphorylation at T187
358 targets p27 to SCF/ Skp2 complex for ubiquitin-dependent degradation (42). CDK2-dependent
359 phosphorylation at T187 and binding of phosphorylated p27 to Skp2 are both considered rate-
360 limiting steps for p27 ubiquitination and subsequent degradation (43, 44). We examined both
361 these events to better define the mechanism of K-Rta mediated up regulation of p27. Figure 7
362 shows the kinetics of Spk2 and p27 phosphorylated at T187 from Dox treated and untreated
363 TRExBJABRta cells at various time intervals following release of cell cycle arrest. Skp2 levels
364 decreased over time with kinetics that parallel increase in the levels of p27 in K-Rta expressing

365 cells. In Dox untreated TRExBJABRta cells, the kinetics was opposite with gradual
366 accumulation of Skp2 over time. In K-Rta expressing cells, there was a decrease in the level of
367 p27 phosphorylation at T187 and a parallel increase in the total p27 levels. However, in Dox
368 untreated cells the level of phosphorylated p27 at T187 gradually increased over time with a
369 parallel decrease in p27 levels as expected. These results suggest that K-Rta mediated up
370 regulation of p27 is most likely a Skp2 dependent event and T187 is the key phosphorylation site
371 targeted.
372 Knock down of p27 expression by shRNAs mitigates K-Rta induced cell cycle arrest. The
373 data above strongly suggest that K-Rta induced cell cycle arrest involved impaired degradation
374 of p27 by Skp2 resulting in accumulation of p27 in the nucleus. To conclusively prove that the
375 observed accumulation of p27 had the causal effect on the cell cycle arrest or is directly
376 responsible for K-Rta mediated cell cycle arrest, we knocked down p27 expression in
377 TRExBJABRta cell line by stably expressing shRNAs against p27. Western blot analysis of Dox
378 treated TRExBJABRta cell lines expressing shRNA against p27 showed efficient but incomplete
379 knock down of p27 expression (~80% in both clones 1 and 2) (Fig. 8A). TRExBJABRta cell
380 lines expressing control shRNAs (Clone 1 and 2) showed no significant reduction in the levels of
381 p27 compared to the parent TRExBJABRta cell line. Next we quantitated cells in G1 phase from
382 TRExBJABRta cells expressing these shRNAs after release from mitotic arrest and treatment
383 with Dox. The results from FACS analysis showed that the down regulation of p27 by shRNA
384 results in a significant decrease in K-Rta induced G1 arrest, ~60% in G1 phase compared to
385 ~70% cells in G1 phase in parent TRExBJABRta cells or TRExBJABRta cells stably expressing
386 control shRNAs (Fig. 8B). We did not observe total abrogation of cell cycle arrest in G1 phase in
387 TRExBJABRta cells expressing shRNA against p27 but we noticed a significant decrease of
388 cells in G1 phase compared to TRExBJABRta cells expressing control shRNA. The data suggest

389 that the accumulation of p27 observed in K-Rta expressing cells contributes to cell cycle arrest at
390 G1.

391 Discussion

392 Our study demonstrates that KSHV encoded immediate early gene K-Rta induces cell
393 cycle arrest in G0/G1 phase in an inducible B-cell line model. Consistent with G1 arrest, K-Rta
394 mediated cell cycle arrest was associated with a decrease in the protein levels for cyclin A and
395 phosphorylated Rb, both markers of S phase progression. Importantly, our results establish p27,
396 a critical cyclin-dependent kinase inhibitor (CDKI) as a key player in K-Rta mediated cell cycle
397 arrest. The central role of p27 in K-Rta mediated G1 arrest is supported by shRNA knockdown
398 of p27, which significantly overrode the cell cycle arrest in K-Rta expressing cells. Since the
399 knockdown of p27 did not completely abolish K-Rta mediated G1 arrest, we cannot exclude the
400 possibility that K-Rta may also be functioning through other pathways that could contribute to
401 cell cycle arrest.

402 Our finding that K-Rta arrests cells in G0/G1 phase is in general agreement with recent
403 studies that investigated the role of EBV encoded Rta (E-Rta) in cell cycle regulation (18). The
404 expression of inducible E-Rta in 293 and nasopharyngeal carcinoma (NPC) derived cells resulted
405 in G1 arrest (18, 19) which was associated with elevated levels of p21 and p27. However, we did
406 not notice any significant changes in the expression of p21 in K-Rta expressing cells. It is
407 possible that E-Rta and K-Rta may have evolved diverse mechanisms to arrest cell cycle in G1
408 phase or these diverse pathways could be due to the different cellular contexts used in the
409 experiments. It is interesting to note that K-Rta mediated increase in p27 levels was not at the
410 transcriptional level and was independent of K-Rta's transactivation ability. The transactivation
411 function of several herpesviral immediate early genes including Zta, IE2 and ICP0 was found to
412 be dispensable for cell cycle arrest (25, 45-47). Instead, the ability to arrest cell cycle was
413 mapped to key motifs that are involved in protein-protein interactions like the bZIP domain of E-
414 Zta and RING finger domain for ICP0 (25, 45). These studies suggest that the transactivation

415 function of immediate early genes may be less important for mediating cell cycle arrest than
416 direct interactions with key cell cycle regulators.

417 In normal cells, p27 levels are maximal in quiescence but falls rapidly as the cells
418 progress from G1 to S phase. p27 is a short-lived protein and its levels are mainly regulated by
419 post-translational proteolytic degradation (39, 48). In the late G1 phase, degradation of p27 is
420 mediated by SCF/Skp2 E3 ubiquitin ligase complex that requires phosphorylation of p27 at T187
421 residue by cyclin E,A/ CDK2 complex (49). The phosphorylation at T187 creates a recognition
422 site for Skp2 complex, which induces p27 poly-ubiquitination and subsequent degradation by the
423 proteasome (41-43). The data presented here demonstrate that p27 was more stable in K-Rta
424 expressing cells. This finding was also supported by decreased poly-ubiquitination of p27
425 observed in K-Rta expressing cells. It is noteworthy that p27 degradation involves both Skp2-
426 dependent and -independent proteosomal degradation pathways (39). We have focused on Skp2-
427 dependent proteosomal pathway, as it is the best-characterized and most potent degradation
428 pathway that determines p27 stability. It remains to be clarified whether K-Rta mediated
429 stabilization of p27 also involve another degradation pathway besides Skp2-dependent pathway
430 that would function independently of T187 phosphorylation.

431 Based on our results, we hypothesize that there are at least three non-mutually exclusive
432 possibilities by which K-Rta can induce cell cycle arrest, as summarized in Figure 8. First, K-Rta
433 may sequester p27 in the nucleus to prevent its export to the cytoplasm by direct or indirect
434 interaction. The localization of p27 seems to be finely regulated during G1 progression (39). To
435 act as a cell cycle inhibitor, p27 must be localized in the nucleus, whereas its cytoplasmic export
436 allows cell cycle progression. In our study we observed the accumulation of p27 in the nucleus
437 of K-Rta expressing cells, but it is difficult to resolve whether K-Rta is directly modulating the
438 subcellular localization of p27 or the nuclear accumulation of p27 is an indirect consequence of

K-Rta mediated cell cycle arrest. The second possibility is that K-Rta may induce or repress the expression of any upstream kinase or phosphatase, which may regulate the phosphorylation of p27. Several key phosphorylation sites have been characterized in recent years including S10, T157 and T198 that determine p27 stability and subcellular localization (39). The third possibility is that K-Rta may directly or indirectly interact with SCF/Skp2 complex to disrupt the binding between p27 and Skp2, which targets p27 for subsequent proteosomal degradation. Since K-Rta has been shown to possess E3 ubiquitin ligase activity, the last scenario becomes particularly interesting if Skp2 is identified as a target for K-Rta-mediated proteosomal degradation (50). In that case p27 will escape Skp2 mediated proteosomal degradation and would accumulate in the nucleus. We were able to co-immunoprecipitate over expressed tagged versions of K-Rta and Skp2 in transiently transfected 293T cells (Data not shown), however our effort to detect this interaction in vivo under physiologically relevant conditions was unsuccessful. It is plausible that the interaction between K-Rta and Skp2 is transient in nature and/or very weak.

Recent research suggests that KSHV lytic reactivation is tightly linked to B-cell terminal differentiation (51). KSHV remains latent in a not very well characterized B-cell compartment until B cells differentiate into plasma cells. This terminal differentiation provides the physiological lytic switch through plasma cell transcription factor X box binding protein 1 (XBP-1s). Thus, KSHV like EBV reactivates by exploiting the terminal differentiation pathway of latently infected B cells. In most cell lineages, final differentiation is associated with loss of proliferation and cell cycle arrest in G1 phase (52). During the differentiation process, the expression of various CDKIs including p27 is up regulated. Strong evidence for a role of p27 in differentiation programs comes from studies in mice lacking p27, which shows altered differentiation program in various tissues (53-55). It would be interesting to investigate whether

463 K-Rta mediated up-regulation of p27 following lytic reactivation also plays a role in
464 differentiation of B cells besides cell cycle arrest.

465 An issue that remains to be resolved is the experimental validation of the hypothesis of
466 the presumed benefit of cell cycle arrest during KSHV or in general herpesvirus lytic replication.
467 Most studies including ours have investigated the role of herpesviral immediate early genes in
468 cell cycle regulation in an over expressed system. Experimental validation in the context of
469 normal viral infection setting proves to be a challenging endeavor, most likely because of
470 temporal and ephemeral nature of cell cycle arrest. In case of KSHV, it has been shown that
471 following K-Rta induction there is a substantial increase in the expression of vCyclin and LANA
472 proteins, both of which have the potential to accelerate cell cycle progression modulating Rb-
473 E2F pathway. Clearly, more work is needed to obtain a comprehensive understanding of cell
474 cycle regulation in herpesvirus lytic replication.

475 In summary our results demonstrate that KSHV encoded K-Rta is another player besides
476 K8 that participate in arresting host cells in G1 phase following viral reactivation. K-Rta
477 mediated cell cycle arrest was associated with stabilization and increased nuclear accumulation
478 of p27. Our study has revealed a discrete functional role for K-Rta in host cell cycle regulation,
479 which is independent of its function as a major viral transcriptional factor.

480 Acknowledgements

481 This work was supported in part by the Public Health Service grants CA-75903, P20
482 RR15635 and P30 GM103509 from the National Institutes of Health.

483 We would like to thank Dr. Levon Abrahamyan for his help with confocal microscopy
484 and Danielle Shea for help with flow cytometry. We also thank Dr. J. U. Jung at the University
485 of Southern California for providing RTA-inducible BJAB cell line, Dr Luwen Zhang at the
486 University of Nebraska, Lincoln for DG75 and Cro6 cell lines and Dr. Izumiya at UC Davis for
487 Rta polyclonal serum.

488 References

489 1. Mesri EA, Cesarman E, Boshoff C. 2010. Kaposi's sarcoma and its associated
490 herpesvirus. Nat Rev Cancer 10:707-719.
491 2. Cesarman E, Chang Y, Moore PS, Said JW, Knowles DM. 1995. Kaposi's sarcoma-
492 associated herpesvirus-like DNA sequences in AIDS-related body-cavity-based
493 lymphomas. N Engl J Med 332:1186-1191.
494 3. Chang Y, Cesarman E, Pessin MS, Lee F, Culpepper J, Knowles DM, Moore PS.
495 1994. Identification of herpesvirus-like DNA sequences in AIDS-associated Kaposi's
496 sarcoma. Science 266:1865-1869.
497 4. Soulier J, Grollet L, Oksenhendler E, Cacoub P, Cazals-Hatem D, Babinet P,
498 d'Agay MF, Clauvel JP, Raphael M, Degos L, Sigaux F. 1995. Kaposi's sarcoma-
499 associated herpesvirus-like DNA sequences in multicentric Castleman's disease. Blood
500 86:1276-1280.
501 5. Ganem D. 2010. KSHV and the pathogenesis of Kaposi sarcoma: listening to human
502 biology and medicine. J Clin Invest 120:939-949.
503 6. Sun R, Lin SF, Gradoville L, Yuan Y, Zhu F, Miller G. 1998. A viral gene that
504 activates lytic cycle expression of Kaposi's sarcoma-associated herpesvirus. Proc Natl
505 Acad Sci U S A 95:10866-10871.
506 7. Lukac DM, Renne R, Kirshner JR, Ganem D. 1998. Reactivation of Kaposi's sarcoma-
507 associated herpesvirus infection from latency by expression of the ORF 50 transactivator,
508 a homolog of the EBV R protein. Virology 252:304-312.
509 8. Gradoville L, Gerlach J, Grogan E, Shedd D, Nikiforow S, Metroka C, Miller G.
510 2000. Kaposi's sarcoma-associated herpesvirus open reading frame 50/Rta protein

511 activates the entire viral lytic cycle in the HH-B2 primary effusion lymphoma cell line. J
512 Virol 74:6207-6212.
513 9. Xu Y, AuCoin DP, Huete AR, Cei SA, Hanson LJ, Pari GS. 2005. A Kaposi's
514 sarcoma-associated herpesvirus/human herpesvirus 8 ORF50 deletion mutant is defective
515 for reactivation of latent virus and DNA replication. J Virol 79:3479-3487.
516 10. Duan W, Wang S, Liu S, Wood C. 2001. Characterization of Kaposi's sarcoma-
517 associated herpesvirus/human herpesvirus-8 ORF57 promoter. Arch Virol 146:403-413.
518 11. Deng H, Young A, Sun R. 2000. Auto-activation of the rta gene of human herpesvirus-
519 8/Kaposi's sarcoma-associated herpesvirus. J Gen Virol 81:3043-3048.
520 12. Deng H, Chu JT, Rettig MB, Martinez-Maza O, Sun R. 2002. Rta of the human
521 herpesvirus 8/Kaposi sarcoma-associated herpesvirus up-regulates human interleukin-6
522 gene expression. Blood 100:1919-1921.
523 13. Chen J, Ueda K, Sakakibara S, Okuno T, Yamanishi K. 2000. Transcriptional
524 regulation of the Kaposi's sarcoma-associated herpesvirus viral interferon regulatory
525 factor gene. J Virol 74:8623-8634.
526 14. Chang PJ, Shedd D, Gradoville L, Cho MS, Chen LW, Chang J, Miller G. 2002.
527 Open reading frame 50 protein of Kaposi's sarcoma-associated herpesvirus directly
528 activates the viral PAN and K12 genes by binding to related response elements. J Virol
529 76:3168-3178.
530 15. Bowser BS, Morris S, Song MJ, Sun R, Damania B. 2006. Characterization of
531 Kaposi's sarcoma-associated herpesvirus (KSHV) K1 promoter activation by Rta.
532 Virology 348:309-327.

16. Salvant BS, Fortunato EA, Spector DH. 1998. Cell cycle dysregulation by human cytomegalovirus: influence of the cell cycle phase at the time of infection and effects on cyclin transcription. J Virol 72:3729-3741.

17. Izumiya Y, Lin SF, Ellison TJ, Levy AM, Mayeur GL, Izumiya C, Kung HJ. 2003. Cell cycle regulation by Kaposi's sarcoma-associated herpesvirus K-bZIP: direct interaction with cyclin-CDK2 and induction of G1 growth arrest. J Virol 77:9652-9661.

18. Huang SY, Hsieh MJ, Chen CY, Chen YJ, Chen JY, Chen MR, Tsai CH, Lin SF, Hsu TY. 2012. Epstein-Barr virus Rta-mediated transactivation of p21 and 14-3-3sigma arrests cells at the G1/S transition by reducing cyclin E/CDK2 activity. J Gen Virol 93:139-149.

19. Chen YL, Chen YJ, Tsai WH, Ko YC, Chen JY, Lin SF. 2009. The Epstein-Barr virus replication and transcription activator, Rta/BRLF1, induces cellular senescence in epithelial cells. Cell Cycle 8:58-65.

20. Flemington EK. 2001. Herpesvirus lytic replication and the cell cycle: arresting new developments. J Virol 75:4475-4481.

21. Nishioka WK, Welsh RM. 1994. Susceptibility to cytotoxic T lymphocyte-induced apoptosis is a function of the proliferative status of the target. J Exp Med 179:769-774.

22. Kawaguchi Y, Van Sant C, Roizman B. 1997. Herpes simplex virus 1 alpha regulatory protein ICP0 interacts with and stabilizes the cell cycle regulator cyclin D3. J Virol 71:7328-7336.

23. Hobbs WE, 2nd, DeLuca NA. 1999. Perturbation of cell cycle progression and cellular gene expression as a function of herpes simplex virus ICP0. J Virol 73:8245-8255.

24. Rodriguez A, Jung EJ, Yin Q, Cayrol C, Flemington EK. 2001. Role of c-myc regulation in Zta-mediated induction of the cyclin-dependent kinase inhibitors p21 and p27 and cell growth arrest. Virology 284:159-169.

25. Cayrol C, Flemington EK. 1996. The Epstein-Barr virus bZIP transcription factor Zta causes G0/G1 cell cycle arrest through induction of cyclin-dependent kinase inhibitors. EMBO J 15:2748-2759.

26. Wu FY, Chen H, Wang SE, ApRhys CM, Liao G, Fujimuro M, Farrell CJ, Huang J, Hayward SD, Hayward GS. 2003. CCAAT/enhancer binding protein alpha interacts with ZTA and mediates ZTA-induced p21(CIP-1) accumulation and G(1) cell cycle arrest during the Epstein-Barr virus lytic cycle. J Virol 77:1481-1500.

27. Wu FY, Wang SE, Tang QQ, Fujimuro M, Chiou CJ, Zheng Q, Chen H, Hayward SD, Lane MD, Hayward GS. 2003. Cell cycle arrest by Kaposi's sarcoma-associated herpesvirus replication-associated protein is mediated at both the transcriptional and posttranslational levels by binding to CCAAT/enhancer-binding protein alpha and p21(CIP-1). J Virol 77:8893-8914.

28. Nakamura H, Lu M, Gwack Y, Souvlis J, Zeichner SL, Jung JU. 2003. Global changes in Kaposi's sarcoma-associated virus gene expression patterns following expression of a tetracycline-inducible Rta transactivator. J Virol 77:4205-4220.

29. Trivedi P, Takazawa K, Zompetta C, Cuomo L, Anastasiadou E, Carbone A, Uccini S, Belardelli F, Takada K, Frati L, Faggioni A. 2004. Infection of HHV-8+ primary effusion lymphoma cells with a recombinant Epstein-Barr virus leads to restricted EBV latency, altered phenotype, and increased tumorigenicity without affecting TCL1 expression. Blood 103:313-316.

30. Shao R, Guo X. 2004. Human microvascular endothelial cells immortalized with human telomerase catalytic protein: a model for the study of in vitro angiogenesis. Biochem Biophys Res Commun 321:788-794.

31. Wen HJ, Yang Z, Zhou Y, Wood C. 2010. Enhancement of autophagy during lytic replication by the Kaposi's sarcoma-associated herpesvirus replication and transcription activator. J Virol 84:7448-7458.

32. Riccardi C, Nicoletti I. 2006. Analysis of apoptosis by propidium iodide staining and flow cytometry. Nat Protoc 1:1458-1461.

33. Livak KJ, Schmittgen TD. 2001. Analysis of relative gene expression data using real-time quantitative PCR and the 2(-Delta Delta C(T)) Method. Methods 25:402-408.

34. Tiscornia G, Singer O, Verma IM. 2006. Production and purification of lentiviral vectors. Nat Protoc 1:241-245.

35. Giacinti C, Giordano A. 2006. RB and cell cycle progression. Oncogene 25:5220-5227.

36. Resnitzky D, Hengst L, Reed SI. 1995. Cyclin A-associated kinase activity is rate limiting for entrance into S phase and is negatively regulated in G1 by p27Kip1. Mol Cell Biol 15:4347-4352.

37. Chang H, Gwack Y, Kingston D, Souvlis J, Liang X, Means RE, Cesarman E, Hutt-Fletcher L, Jung JU. 2005. Activation of CD21 and CD23 gene expression by Kaposi's sarcoma-associated herpesvirus RTA. J Virol 79:4651-4663.

38. Pagano M, Tam SW, Theodoras AM, Beer-Romero P, Del Sal G, Chau V, Yew PR, Draetta GF, Rolfe M. 1995. Role of the ubiquitin-proteasome pathway in regulating abundance of the cyclin-dependent kinase inhibitor p27. Science 269:682-685.

39. Susaki E, Nakayama KI. 2007. Multiple mechanisms for p27(Kip1) translocation and degradation. Cell Cycle 6:3015-3020.

40. Reynisdottir I, Massague J. 1997. The subcellular locations of p15(Ink4b) and p27(Kip1) coordinate their inhibitory interactions with cdk4 and cdk2. Genes Dev 11:492-503.

41. Carrano AC, Eytan E, Hershko A, Pagano M. 1999. SKP2 is required for ubiquitin-mediated degradation of the CDK inhibitor p27. Nat Cell Biol 1:193-199.

42. Tsvetkov LM, Yeh KH, Lee SJ, Sun H, Zhang H. 1999. p27(Kip1) ubiquitination and degradation is regulated by the SCF(Skp2) complex through phosphorylated Thr187 in p27. Curr Biol 9:661-664.

43. Malek NP, Sundberg H, McGrew S, Nakayama K, Kyriakides TR, Roberts JM. 2001. A mouse knock-in model exposes sequential proteolytic pathways that regulate p27Kip1 in G1 and S phase. Nature 413:323-327.

44. Nakayama K, Nagahama H, Minamishima YA, Miyake S, Ishida N, Hatakeyama S, Kitagawa M, Iemura S, Natsume T, Nakayama KI. 2004. Skp2-mediated degradation of p27 regulates progression into mitosis. Dev Cell 6:661-672.

45. Lomonte P, Everett RD. 1999. Herpes simplex virus type 1 immediate-early protein Vmw110 inhibits progression of cells through mitosis and from G(1) into S phase of the cell cycle. J Virol 73:9456-9467.

46. Rodriguez A, Armstrong M, Dwyer D, Flemington E. 1999. Genetic dissection of cell growth arrest functions mediated by the Epstein-Barr virus lytic gene product, Zta. J Virol 73:9029-9038.

47. Wiebusch L, Hagemeier C. 1999. Human cytomegalovirus 86-kilodalton IE2 protein blocks cell cycle progression in G(1). J Virol 73:9274-9283.

48. Vervoorts J, Luscher B. 2008. Post-translational regulation of the tumor suppressor p27(KIP1). Cell Mol Life Sci 65:3255-3264.

626 49. Montagnoli A, Fiore F, Eytan E, Carrano AC, Draetta GF, Hershko A, Pagano M.
627 1999. Ubiquitination of p27 is regulated by Cdk-dependent phosphorylation and trimeric
628 complex formation. Genes Dev 13:1181-1189.
629 50. Yu Y, Wang SE, Hayward GS. 2005. The KSHV immediate-early transcription factor
630 RTA encodes ubiquitin E3 ligase activity that targets IRF7 for proteosome-mediated
631 degradation. Immunity 22:59-70.
632 51. Wilson SJ, Tsao EH, Webb BL, Ye H, Dalton-Griffin L, Tsantoulas C, Gale CV, Du
633 MQ, Whitehouse A, Kellam P. 2007. X box binding protein XBP-1s transactivates the
634 Kaposi's sarcoma-associated herpesvirus (KSHV) ORF50 promoter, linking plasma cell
635 differentiation to KSHV reactivation from latency. J Virol 81:13578-13586.
636 52. Kaldis P, Richardson HE. 2012. When cell cycle meets development. Development
637 139:225-230.
638 53. Durand B, Gao FB, Raff M. 1997. Accumulation of the cyclin-dependent kinase
639 inhibitor p27/Kip1 and the timing of oligodendrocyte differentiation. EMBO J 16:306-
640 317.
641 54. Kiyokawa H, Kineman RD, Manova-Todorova KO, Soares VC, Hoffman ES, Ono
642 M, Khanam D, Hayday AC, Frohman LA, Koff A. 1996. Enhanced growth of mice
643 lacking the cyclin-dependent kinase inhibitor function of p27(Kip1). Cell 85:721-732.
644 55. Nakayama K, Ishida N, Shirane M, Inomata A, Inoue T, Shishido N, Horii I, Loh
645 DY. 1996. Mice lacking p27(Kip1) display increased body size, multiple organ
646 hyperplasia, retinal dysplasia, and pituitary tumors. Cell 85:707-720.
647
648
649

650 Figure Legends

651 Figure 1. KSHV reactivation following TPA treatment arrests cells in G0/G1 phase:
652 Asynchronously growing exponential cultures of BC3 and Cro6 (KSHV positive) and DG75
653 (KSHV negative) cells were treated with TPA (20 ng/ml). At the indicated times post-TPA
654 treatment, the cells were fixed, stained with propidium iodide (PI) and analyzed by flow
655 cytometry. Cell cycle phase distribution was determined using ModFit LT version 2.0 software.
656 Cell cycle profiles presented here are representative of two independent experiments.

657 Figure 2. K-Rta arrests cells in G0/G1 phase: (A) Asynchronously growing exponential
658 cultures of control cell line (TRExBJAB) and Rta inducible BJAB cell line (TRExBJABRta)
659 were synchronized by serum starvation for 24 hours. Growth arrested cells were stimulated with
660 medium containing 10% serum and doxycycline (Dox). At the indicated times post-Dox
661 treatment, the cells were fixed, stained with propidium iodide (PI) and analyzed by flow
662 cytometry. Cell cycle phase distribution was determined using ModFit LT version 2.0 software.
663 Data represents the mean of three independent experiments. Errors bars represent SD for
664 triplicate samples. A significant increase in the number of cells stuck at G0/G1 phase was noted
665 in TRExBJAB vs TRExBJABRta at 48 hrs ($p=0.006$) and 72 hrs ($p<0.001$) post-Dox treatment.
666 (B) Asynchronously growing exponential cultures of TREx293 Rta cells were treated with
667 doxycycline. At 72 hrs post-Dox treatment, treated and untreated cells were fixed, stained with
668 PI and cell cycle status was determined by flow cytometry as described above. A significant
669 arrest in G1 phase was noted for Dox treated TREx293Rta cells at 72 hrs post Dox treatment
670 compared to untreated cells ($p<0.001$). Cell cycle profiles presented here are mean of three
671 independent experiments. Errors bars represent SD for triplicate samples.

672 Figure 3. K-Rta expressing cells have increased levels of $p27^{kip1}$: (A) Asynchronously
673 growing exponential cultures of control cell line (TRExBJAB) and Rta inducible BJAB cell line

674 (TRExBJABRta) were synchronized by serum starvation for 24 hours. Growth arrested cells
675 were stimulated with medium containing 10% serum and doxycycline. Doxycycline treated or
676 untreated TRExBJAB and TRExBJABRta cells were harvested and the expression kinetics of
677 key cell cycle regulators were followed by immunoblotting at indicated times. GAPDH served as
678 a loading control. The numbers below p27 band indicate the relative intensities of the p27 protein
679 normalized to GAPDH protein. (B) Asynchronously growing DG75 (KSHV negative) and BC3
680 (KSHV positive) cells were treated with TPA (20 ng/ml) for 24 and 48 hrs. The lysates were
681 immunoblotted with antibodies as indicated. (C) DG75 and Vero cells were transiently
682 transfected with either empty Flag vector or Flag Rta expression plasmid. Human Microvascular
683 Endothelial Cells (HMVEC) cells were transduced with equal amounts of either control
684 lentivirus or lentivirus expressing K-Rta. The cells were harvested after 36 hrs and the lysates
685 were immunoblotted with antibodies as indicated. The values below the figure represent relative
686 density of p27 bands normalized to that of GAPDH bands.
687 Figure 4. K-Rta does not affect p27 at the transcriptional level: (A) RNA was harvested
688 from parallel samples collected at 0, 24, 48 and 72 hrs from doxycycline treated or untreated
689 TRExBJAB and TRExBJABRta cells from the same experiment as described in Fig 2. The
690 samples were subjected to quantitative real-time PCR analysis to detect the transcript levels of
691 K-Rta, p27 and GAPDH. Each sample was tested in triplicate and representative data obtained
692 from two independent experiments is shown. Relative gene expression was normalized to
693 GAPDH expression and the fold change in the expression of each gene was calculated by using
694 the delta-delta Ct method. (B) Schematic diagram depicting various domains of Rta protein.
695 $5X10^6$ 293-T cells were transiently transfected with 4 µg of either empty Flag vector, Flag vector
696 expressing full length K-Rta (FL) or Flag vector expressing truncated K-Rta (1-527 AA). The
697 cells were harvested 36 hrs post transfection and whole cell lysate was immunoblotted with anti-

698 Flag antibody, anti-p27 antibody and anti-GAPDH antibody. LZ – Leucine zipper, NLS –
699 Nuclear localization signal.
700 Figure 5. K-Rta affects p27 protein stability: (A) Stability test: K-Rta inducible BJAB cell
701 cultures (TRExBJABRta) were treated with 50 μg/ml cyclohexamide (CHX) in the absence or
702 presence of doxycycline (Dox) for indicated lengths of time (In hours). Cell lysates were
703 subjected to Western blot analysis with indicated antibodies. The relative band intensity of p27
704 (normalized to GAPDH) was plotted with respect to time after CHX addition. Gel images
705 presented here are representative of three independent experiments. (B) Doxycyline treated and
706 untreated (for 48 hrs) TRExBJABRta cells were pretreated with proteasome inhibitor MG132
707 (20 μM) before harvesting. Cell extracts were prepared under denaturing lysis conditions and
708 p27 was immunoprecipitated (IP) from Dox treated and untreated TRExBJABRta cells.
709 Immunoprecpitates were subjected to Western blot analysis using p27, Rta and GAPDH
710 antibody. The same membrane was stripped and reprobed with anti-Ubiquitin (Ub) antibody. Gel
711 images presented here are representative of three independent experiments. WB – Western Blot.
712 Figure 6. K-Rta can promote nuclear localization of p27: (A) TRExBJABRta cells were
713 treated with doxycycline for 48 hrs. The Dox treated and untreated cells were fixed with 4%
714 paraformaldehyde for 20 min, permeabilized with 0.2% Triton X-100 in PBS for 10 minutes, and
715 blocked for 30 min with 2% bovine serum albumin (BSA) in PBS. After incubation with primary
716 antibodies (anti-p27 and anti-Rta, both 1:250 dilution) in 2% BSA for 2 hrs at room temperature,
717 the cells were incubated with anti-mouse Alexa-Fluor-488 and anti-rabbit Alexa-Fluor-647
718 conjugated secondary antibodies (1:1000) for 1 hour at room temperature. The Rta and p27
719 localization and DAPI stained nuclei were visualized by confocal microscopy. (B) Cytosolic and
720 nuclear fractions were extracted from TRExBJABRta cells treated with doxycyline and subjected
721 to western blotting with indicated antibodies. TATA binding protein (TBP) and α-tubulin were

used as a nuclear fraction and cytosolic fraction loading control respectively. The bar graph on the right side shows percent of p27 quantitated in the nuclear fraction (normalized to total p27 levels). Gel images presented here are representative of two independent experiments.

Figure 7. K-Rta expressing cells have decreased levels of Skp2: TRExBJABRta cells were serum starved for 24 hours. Growth arrested cells were stimulated with medium containing 10% serum and doxycycline. At times indicated doxycycline treated and untreated cells were harvested and lysates were subjected to immunoblot analysis with indicated antibodies. GAPDH served as a loading control. Gel images presented here are representative of two independent experiments.

Figure 8. Knock down of p27 expression by sh-RNAs attenuates K-Rta induced cell cycle arrest: The parent cell line, TRExBJABRta cells or TRExBJABRta cells stably expressing control sh-RNA (clone #1 and #2) or sh-RNA against p27 (clone #1 and #2) were serum starved for 24 hrs. Growth arrested cells were stimulated with medium containing 10% serum and doxycycline. At 48 hrs post doxycycline treatment, the cells were harvested for flow cytometry and immunoblot analysis. (A) Whole cell lysates were subjected to immunoblot analysis with indicated antibodies. GAPDH served as a loading control. The numbers below p27 band indicate the relative intensities of the p27 protein normalized to GAPDH protein. (B) For flow cytometry, the cells were fixed, stained with propidium iodide and cell cycle phase distribution was determined using ModFit LT version 2.0 software. Data represents the mean ± SD of two independent experiments.

Figure 9. A schematic diagram for K-Rta mediated cell cycle arrest in G0/G1 phase: 1, 2 and 3 represent alternate possibilities elaborated in the discussion section by which K-Rta can induce cell cycle arrest.

Figure 1.

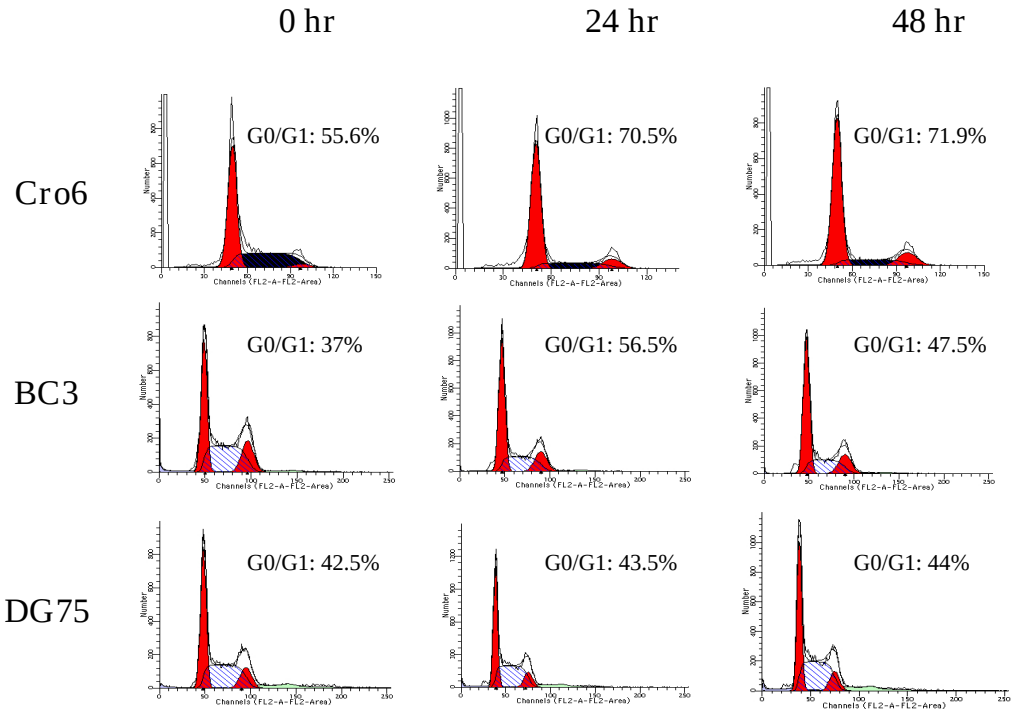

Figure 2.

A

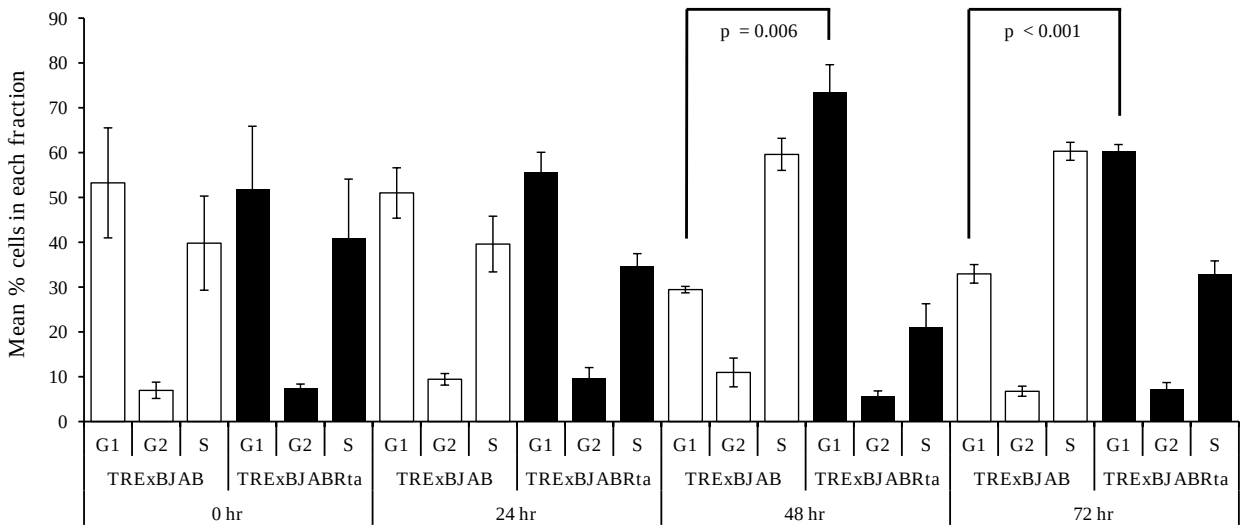

B

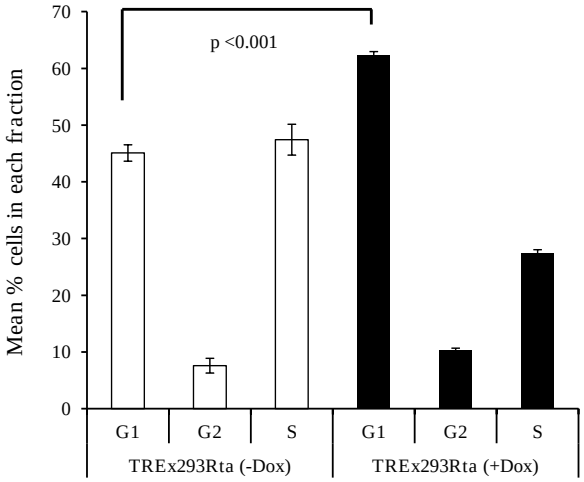

Figure 3.

A

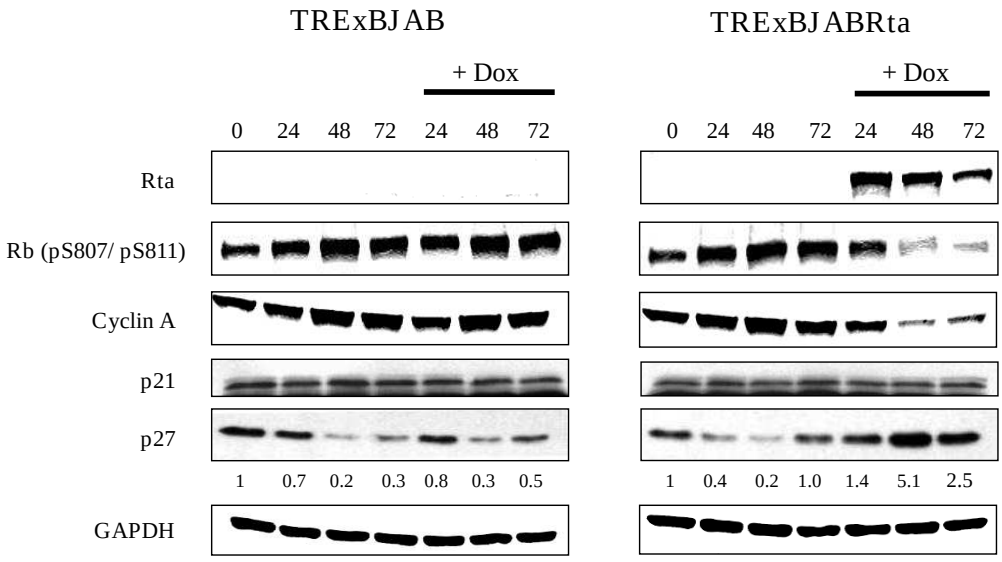

B

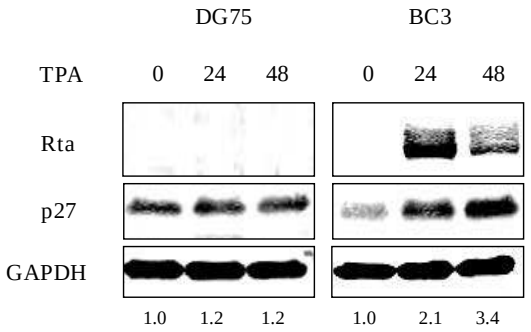

C

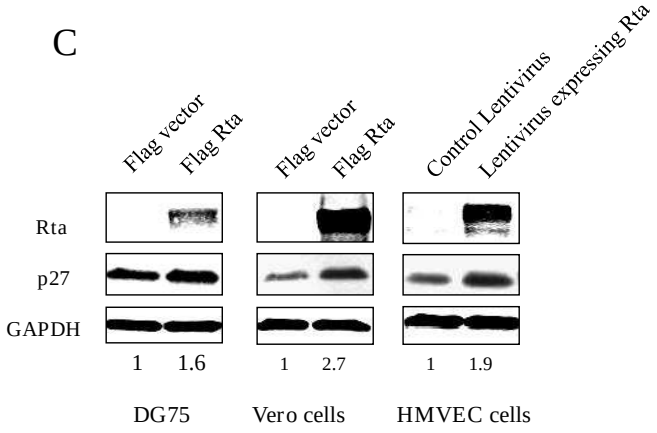

Figure 4.

A

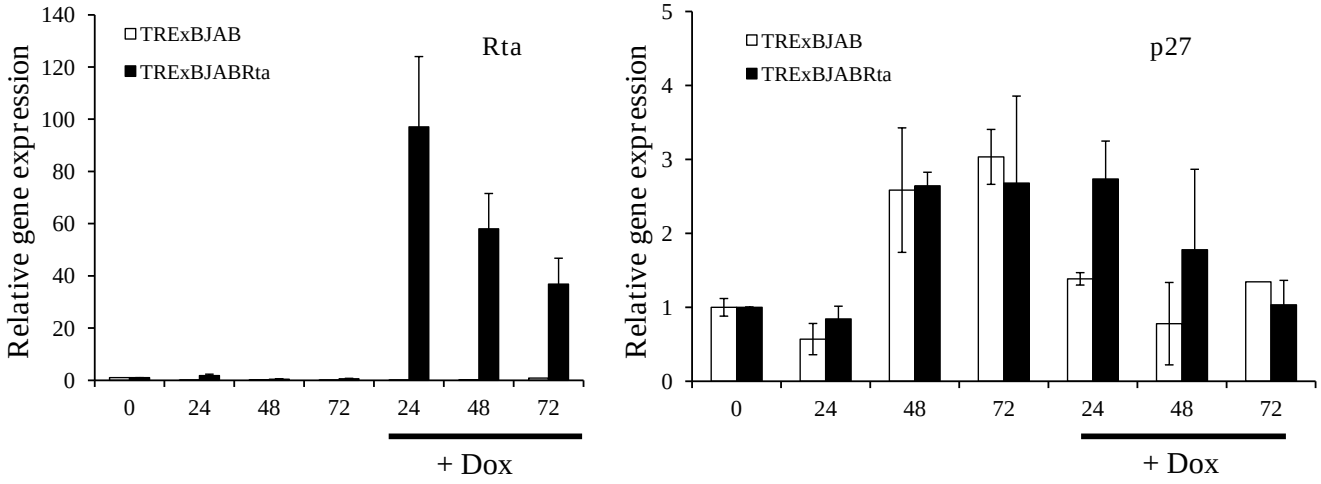

B

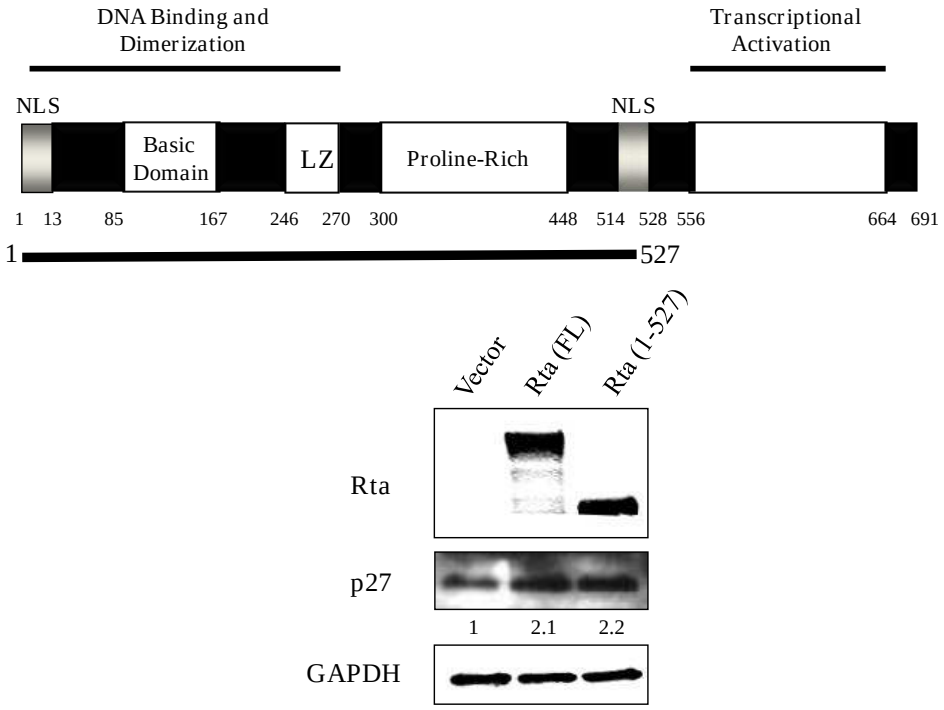

Figure 5.

A

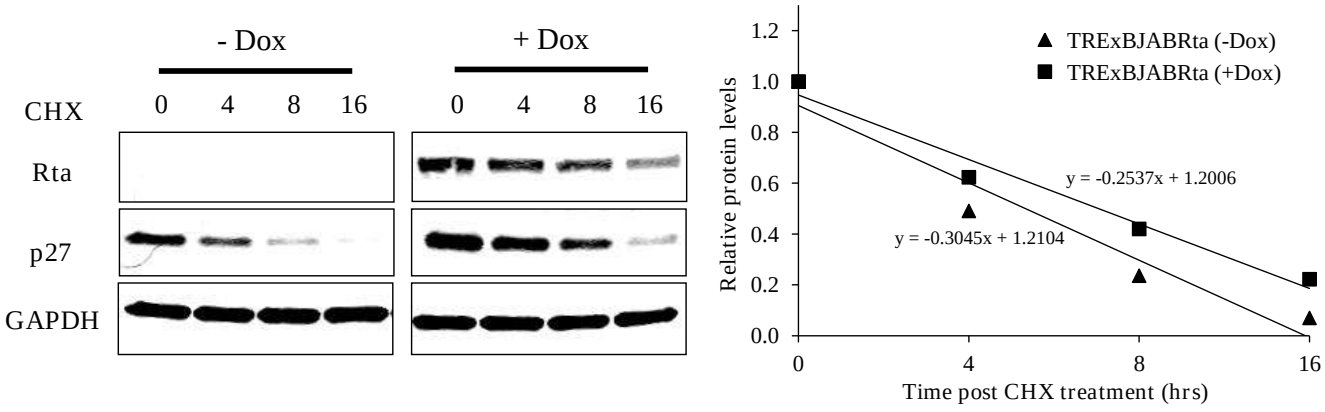

B

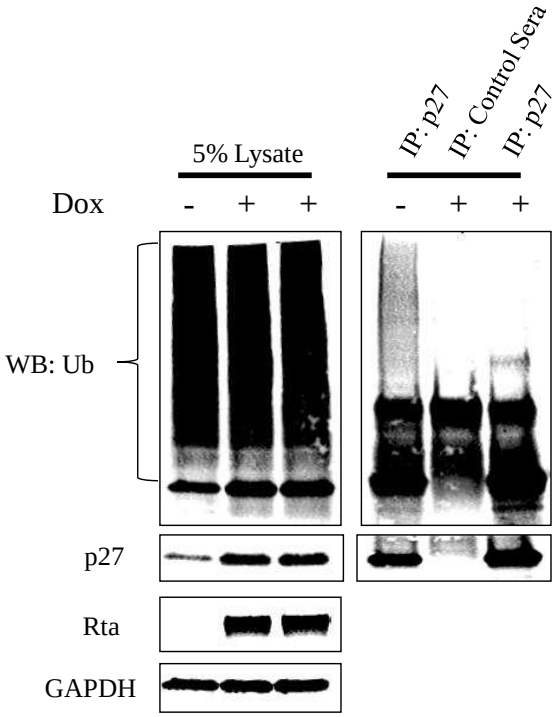

Figure 6.

A

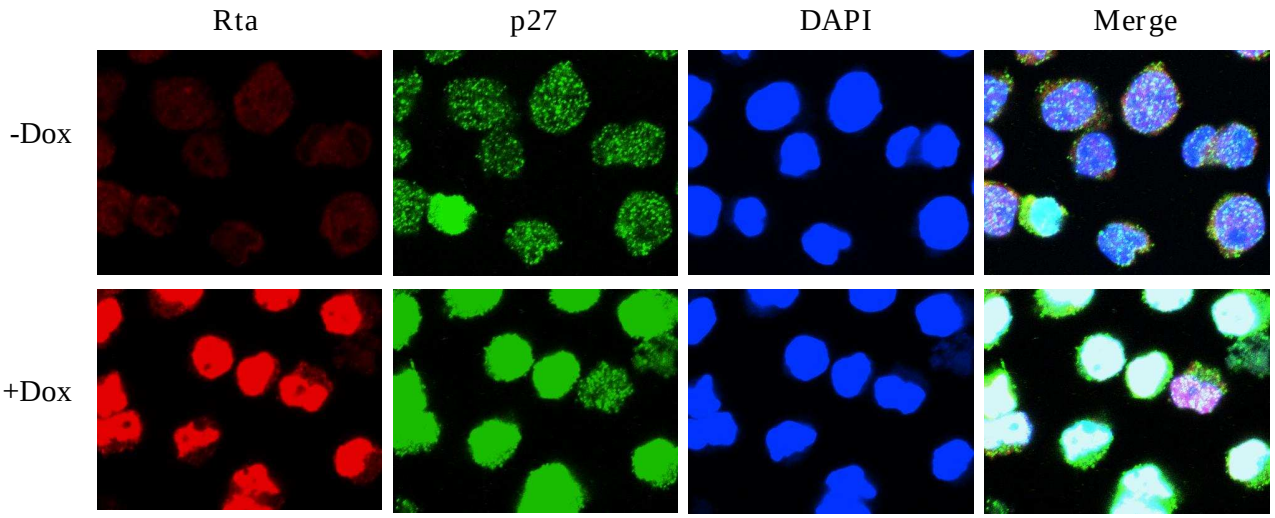

B

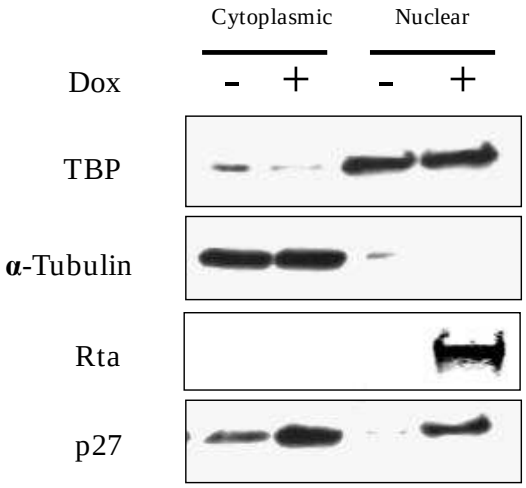

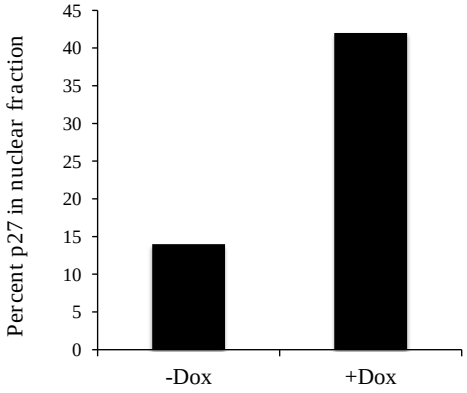

Figure 7.

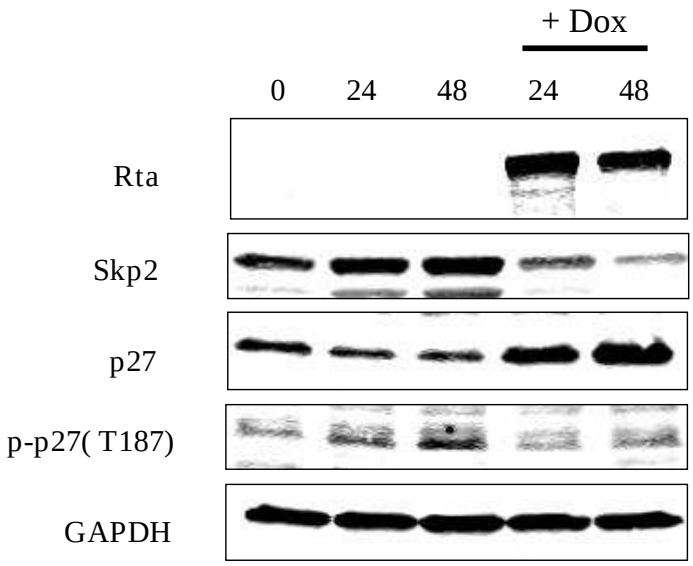

Figure 8.

A

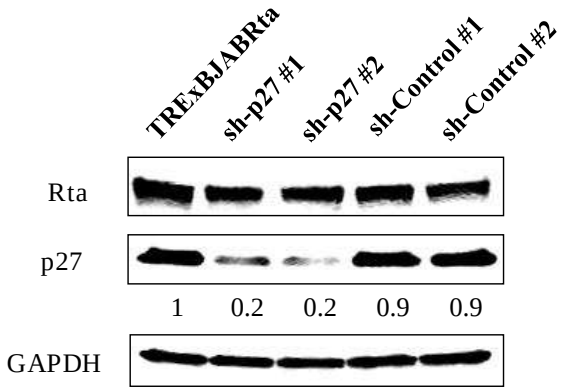

B

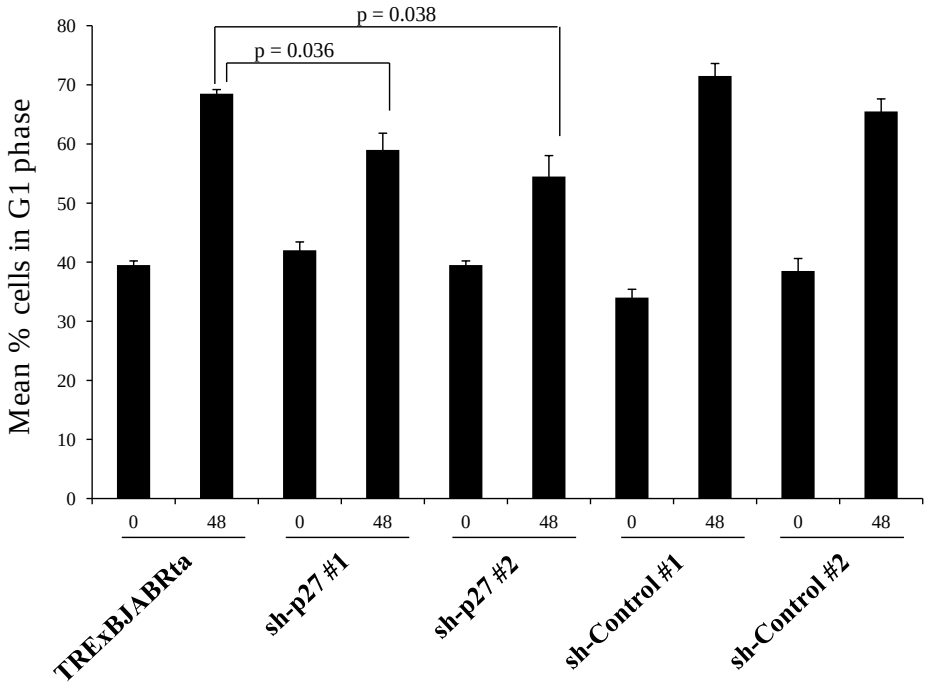

Figure 9.